Land-Use and Land-Cover Change, Urban Heat Island Phenomenon, and Health Implications: A Remote Sensing Approach

C.P. Lo and Dale A. Quattrochi

Abstract

Land-use and land-cover maps of Atlanta Metropolitan Area in Georgia were produced from Landsat MSS and TM images for 1973, 1979, 1983, 1987, 1992, and 1997, spanning a period of 25 years. Dramatic changes in land use and land cover have occurred, with loss of forest and cropland to urban use. In particular, low-density urban use, which includes largely residential use, has increased by over 119 percent between 1973 and 1997. These land-use and land-cover changes have drastically altered the land surface characteristics. An analysis of Landsat images revealed an increase in surface temperature and a decline in NDVI from 1973 to 1997. These changes have forced the development of a significant urban heat island effect at both the urban canopy and urban boundary layers as well as an increase in ground level ozone production to such an extent that Atlanta has violated EPA's ozone level standard in recent years. Using canonical correlation analysis, surface temperatures and NDVI, extracted from Landsat TM images, were found to correlate strongly with volatile organic compounds (VOC) and nitrogen oxides (NOx) emissions, the two ingredients that form ozone by reacting with sunlight, but only weakly with the rates of cardiovascular and chronic lower respiratory diseases, which also did not exhibit strong correlation with VOC and NOx emissions, possibly because other factors such as demographic and socio-economic may also be involved. Further research is therefore needed to understand the health geography and its relationship to land-use and land-cover change. This paper illustrates the usefulness of a remote sensing approach for this purpose.

Introduction

Urbanization is a major event in human history. In the year 2000 it was estimated by the United Nations Population Division that the world's urban population had reached 2.9 billion, or 47 percent of the world's 6.1 billion population, and is expected to rise to 4.9 billion by 2030 or 60 percent of the world's total population. Urban growth and sprawl have drastically altered the biophysical environment. The most noteworthy is the replacement of soil and vegetation with impervious urban materials, such as concrete, asphalt, and buildings, which affect the albedo and runoff characteristics of the land surface, thus significantly impacting the local and regional land-atmosphere energy exchange processes.

In the United States, urbanization has been encouraged by the expansion or development of areas non-adjacent to the traditional downtown urban centers. These are areas of emerging residential, commercial, service-oriented, or industrial development at the periphery of the central city core, thus encroaching on the forested or agricultural hinterlands surrounding the city. Such growth in the "periurban" fringe has resulted in a loss of 2,226 ha of farm and open space in the United States each day, which has profoundly modified the character and state of the Earth's surface (Kostmayer, 1989). A most noticeable phenomenon that has arisen as a result of city expansion is that urban climates are warmer and more polluted than their rural counterparts. This is because the low values of albedo, vegetative cover, and moisture availability in combination with the presence of high levels of anthropogenic heating have given rise to a phenomenon known as the urban heat island (UHI) effect. Hence, urban areas generally act as islands of elevated temperature relative to the natural areas surrounding them (Sailor, 1995). The higher temperatures in the city brought about by UHI have adversely affected air quality because ground level ozone is produced from volatile organic compounds (VOC) in the presence of nitrogen oxides (NOx) and sunlight by a complex set of chemical reactions known as the photochemical smog mechanism (Cardelino and Chameides, 1990). VOC and NOx are emitted from motor vehicles, power plants, and other sources of combustion involving fossil fuel. Ground level ozone is a public health hazard that can cause respiratory and cardiovascular illness. Additionally, the UHI is seen as a possible contributor to increased instances of human mortality during high heat events. In heat waves such as that which occurred in July 1995 over Chicago, Illinois where approximately 525 people died as a result of heat stress, the UHI has been implicated as a major factor in these mortalities (MMWR, 1995; Changnon *et al.*, 1996).

In this paper, the impact of land-use and land-cover change in the city of Atlanta for the past 30 years on urban heat island development, environmental quality, and health implications is reported based on the research conducted under Project ATLANTA (Atlanta Land-use ANalysis: Temperature and Airquality) funded by NASA from 1996 to 2000. A remote sensing approach has been adopted for this research.

C.P. Lo is with the Department of Geography, University of Georgia, Athens, GA 30602 (chpanglo@uga.edu).

D.A. Quattrochi, NASA, Earth Science Department, SD60, Marshall Space Flight Center, AL 35812 (dale.quattrochi@nasa.gov).

Photogrammetric Engineering & Remote Sensing
Vol. 69, No. 9, September 2003, pp. 1053–1063.

0099-1112/03/6909–1053$3.00/0

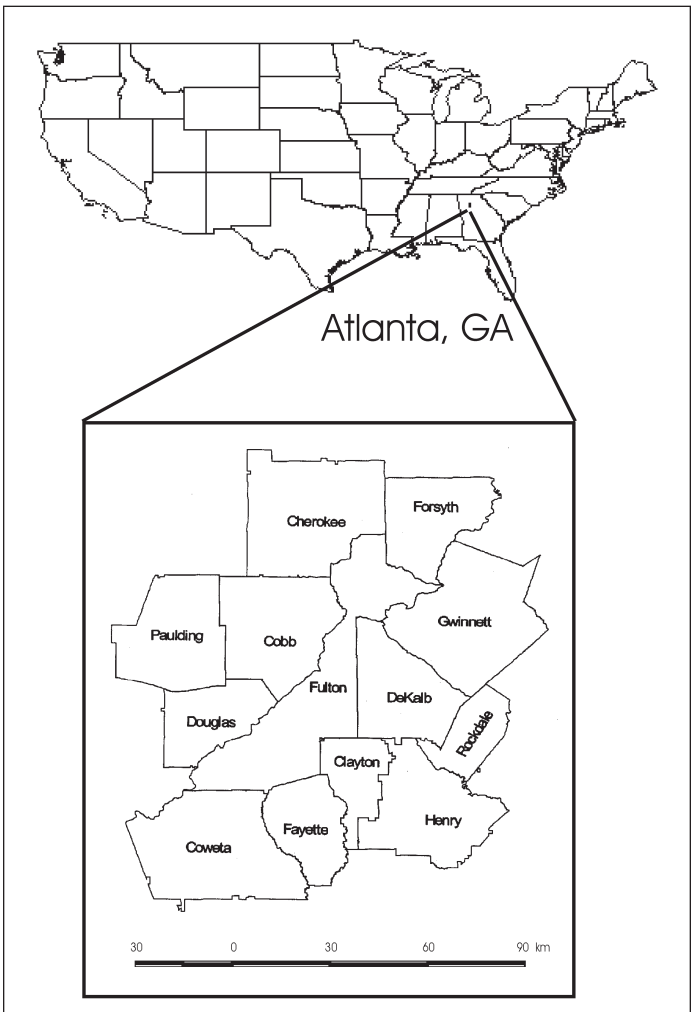

Figure 1. The location of the Atlanta metropolitan area and its 13 urban counties.

Study Area

The metropolitan area of Atlanta, Georgia is an ideal study area for this research because it is the typical American city that has undergone rapid "periurban" growth, as explained above, in the past 30 years. As it emerged to become the premier commercial, industrial, and transportation center of the South, Atlanta's population increased 27 percent between 1970 and 1980, and 33 percent between 1980 and 1990 (Research Atlanta, Inc., 1993). The city has expanded considerably outward from its original city boundaries, located between the counties of DeKalb and Fulton. In this study, the metropolitan area of Atlanta is defined by 13 counties: Cherokee, Clayton, Cobb, DeKalb, Douglas, Fayette, Fulton, Gwinnett, Henry, Rockdale, Coweta, Forsyth, and Paulding (Figure 1).

Land-Use and Land-Cover Mapping

For this project, eleven predominantly cloud-free Landsat scenes of the Atlanta region between 1973 and 1998 were employed. Eight of these are Landsat MSS scenes obtained in 1973, 1979, 1983, 1987, 1988, and 1992, while the remaining three are Landsat TM scenes acquired in 1987, 1997, and 1998 (Table 1). Spring or earlier summer (April through July), when vegetation is in the stage of vigorous growth, is the preferred season for the Landsat scenes.

Reference data used in this study mainly include the color-infrared aerial photographs at a nominal scale of 1:40,000 obtained at the same time as data from NASA's Advanced Thermal and Land Applications Sensor (ATLAS) on 11 May 1997; contact prints of black-and-white and color aerial photographs for the period 1986 through 1988 at a nominal scale of 1:40,000; USGS digital orthophoto quads (DOQs) derived from National Aerial Photography Program (NAPP) photographs taken in January and February of 1993 with a ground resolution of 1 meter and a nominal scale of 1:12,000; a land-cover map of Georgia 1988–1990 generated by ERDAS, Inc. for the Georgia Department of Natural Resources with a nominal scale of 1:24,000 and a 100 ft (30-meter) resolution; and USGS Levels I and II land-use digital maps derived from the original source material from 1972 through 1976 at a scale of 1:250,000.

Before land-use and land-cover mapping can be conducted, some image pre-processing has to be carried out. This includes registering all the Landsat images to the 1997 Landsat TM image, which has already been rectified and georeferenced to the UTM coordinate system (Zone 16), NAD83 horizontal datum, and GRS80 ellipsoid. The Landsat TM and MSS images were resampled to a spatial resolution of 25 meters and 57 meters, respectively, using the nearest-neighbor method and a first-degree polynomial equation. The root-mean-square errors (RMSE) of registration of all these images varied from a low of 0.27 pixel to a high of 0.61 pixel, with the MSS data giving the worst results (Table 1).

Because the Landsat MSS and TM images were acquired by three different generations of sensors at different dates, radiometric normalization had to be carried out to minimize ra-

TABLE 1. CHARACTERISTICS OF THE SATELLITE DATA USED FOR LAND-USE/LAND-COVER CHANGE MAPPING IN THE ATLANTA METROPOLITAN AREA

Date	Type of Imagery	Landsat No.	Nominal Spatial Resolution (m)	Sun Elevation (degree)	Sun Azimuth (degree)	Scene Location	Rectification RMSE (Control Point No.)	Radiometric Normalization
13 Apr 1973	MSS	1	79	54.16	129.37	North Atlanta	0.58 (13)	Yes
13 Apr 1973	MSS	1	79	54.83	127.39	South Atlanta		
11 Jun 1979	MSS	3	79	61.65	105.65	North Atlanta	0.46 (13)	Yes
11 Jun 1979	MSS	3	79	61.74	102.77	South Atlanta		
09 May 1983	MSS	4	79	60.50	117.64	center_shifted*	0.61 (13)	Yes
29 Jun 1987	MSS	5	79	61.84	103.71	center_shifted*	0.44 (13)	No
29 Jun 1987	TM	5	30	61.84	103.71	center_shifted*	0.22 (13)	No
14 May 1988	MSS	5	79	61.61	115.51	center_shifted*	0.51 (12)	reference
23 Apr 1992	MSS	5	79	56.00	121.80	center-shifted*	0.47 (15)	Yes
29 Jul 1997	TM	5	30	61.00	106.00	center_shifted*	reference	No
02 Jan 1998	TM	5	30	27.00	150.00	center_shifted*	0.27 (14)	No

*The center of the north scene has been shifted 50 percent. The scene size is approximately 185 by 185 km.

TABLE 2. LAND-USE AND LAND-COVER CHANGE FOR THE ATLANTA METROPOLITAN AREA (THIRTEEN COUNTIES) AS EXTRACTED FROM LANDSAT IMAGES, 1973–1997/98

Classification Map		High-Density Urban Use	Low-Density Urban Use	Cultivated/ Exposed Land	Cropland/ Grassland	Forest	Water	Total
13 Apr 1973	hectares	45423	121448	9949	198146	653729	15607	1044303
	percent	4.35	11.63	0.95	18.97	62.60	1.49	100.00
11 Jun 1979	hectares	45672	159082	19914	168748	634896	15985	1044298
	percent	4.37	15.23	1.91	16.16	60.80	1.53	100.00
09 May 1983	hectares	61234	171368	20580	161747	613989	15317	1044236
	percent	5.86	16.41	1.97	15.49	58.79	1.47	99.99
29 Jun 1987	hectares	74038	180740	18669	154939	599973	15944	1044303
	percent	7.09	17.31	1.79	14.84	57.45	1.53	100.00
23 Apr 1992	hectares	83987	232009	19655	137428	553746	17477	1044303
	percent	8.04	22.22	1.88	13.16	53.03	1.67	100.00
29 Jul 1997/ 02 Jan 1998	hectares	86027	266222	21552	132168	516987	21347	1044303
	percent	8.24	25.49	2.06	12.66	49.51	2.04	100

diometric differences caused by sensor variations and changes in sensor-target-illumination geometry. After a thorough investigation (Yang and Lo, 2000), the relative radiometric normalization (RRN) method developed by Hall *et al.* (1991) was used.

For this project, the following six-class land-use and land-cover classification scheme was adopted with the main focus on differentiating between urban and non-urban uses: (1) high-density urban use, (2) low-density urban use, (3) cultivated/exposed land, (4) cropland or grassland, (5) forest, and (6) water. Each class is defined by its image characteristics. An unsupervised approach known as ISODATA (Iterative Self-Organizing Data Analysis) was adopted for image classification. It makes use of the minimum-distance method to identify homogeneous spectral clusters iteratively according to the number of clusters specified (Jensen, 1996). In this study, sixty clusters were found to be the optimum for both the Landsat MSS and TM data. All four bands of radiometrically normalized MSS data and six bands (excluding band 6, the thermal-infrared band) of TM data were used in ISODATA clustering.

Using the reference data and visual examination of the false-color composite of the classified Landsat images, the spectral clusters were assigned into one of the six land-use/land-cover classes. Although this approach is labor-intensive, it ensures a high degree of accuracy of the land-use and land-cover maps that can be achieved for use in change detection by the post-classification comparison method. Boundary errors caused by spectral mixing within a pixel as well as spectral confusion due to the similarity of spectral signatures of several land-use and land-cover classes have all been corrected.

Accuracy assessment was performed for the 1988 and the 1997/1998 land-use/land-cover maps only. Based on a stratified random sample of 631 pixels selected from the 1988 map, an overall accuracy of 87 percent was obtained. In terms of producer's and user's accuracies, a minimum of 80 percent was reached for all six classes. As for the 1997/1998 land-use and land-cover map produced, a stratified random sample of 488 pixels revealed an overall accuracy of 90 percent. Both producer's and user's accuracies were over 80 percent. Therefore, the two land-use and land-cover maps were comparable in accuracy despite differences in the type of Landsat images used. The land-use and land-cover classification procedures are more fully explained in Yang and Lo (2002).

Land-Use and Land-Cover Change in Atlanta, 1973 through 1998

The change analysis presented in this paper is based on the statistics extracted from the six land-use/land-cover maps of the Atlanta Metropolitan regions produced for the following dates: (1) 13 April 1973, (2) 11 January 1979, (3) 09 May 1983, (4) 29 June 1987, (5) 23 April 1992, and (6) 10 July 1997/ 02 January 1998 (Plate 1 and Table 2).

It is clearly revealed that the greatest change occurred in the high-density and low-density land-use classes. High-density urban use (which is mostly commercial and industrial in nature) has increased its area from 45,423 hectares (or 4.35 percent) in 1973 to 86,027 hectares (or 8.24 percent) in 1997/1998, or an increase of 89.39 percent (Table 2). Similarly, low-density urban use (which is mostly residential in nature) has increased its area from 121,448 hectares (or 11.63 percent) in 1973 to 266,222 hectares (or 25.49 percent) in 1997/1998, or an increase of 119.21 percent. Spatially, the high-density urban use exhibited a tendency to extend along major highways (notably Interstate Highways 75 and 85), particularly in the northwestern and northeastern parts of the city, from the old city area, while low-density urban use spread to the "peri-urban" fringe, following the high-density urban use. A lot of in-filling occurred within the low-density urban use areas.

The increase in urban use is clearly at the expense of forest and cropland. In 1973, there were 653,729 hectares of forest land (or 62.60 percent), which declined to 516,987 hectares (or 49.51 percent) by 1997/1998, or a decrease of 20.92 percent (Table 2). Similarly, cropland/grassland has declined in area from 198,146 hectares (or 18.97 percent) in 1973 to 132,168 hectares (or 12.66 percent) in 1997/1998, or a decrease of 33.30 percent. Land-use and land-cover statistics have also been extracted at the county level. They revealed that, between 1973 and 1997/1998, the following three counties experienced the highest increase in urban use: Clayton, Cobb, and Gwinnett (Table 3). These counties have also exhibited the highest loss of forest, and, with the exception of Gwinnett, also the highest loss of cropland (Table 3). Gwinnett was one of the fastest growing counties in the United States. It should be noted that Atlanta Airport is located in Clayton county, which explained the large decrease in vegetative cover that has occurred as the Airport expanded through these years.

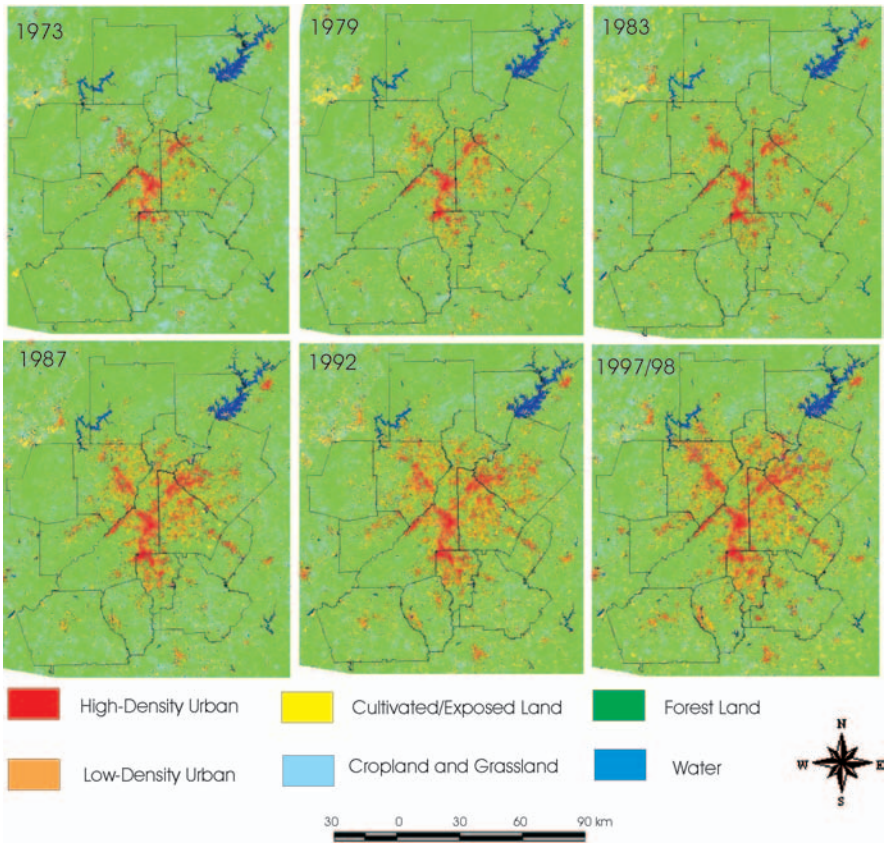

Plate 1. Land-use and land-cover maps of the 13 urban counties of Atlanta as extracted from Landsat images.

TABLE 3. PERCENTAGE OF LAND-USE AND LAND-COVER CHANGE BY COUNTIES, ATLANTA, 1973–1997/98

County	High-Density Urban Use	Low-Density Urban Use	Cultivated/ Exposed Land	Cropland or Grassland	Forest	Water
Cherokee	2.06	9.27	1.04	−0.84	−11.88	0.34
Clayton	9.69	17.87	−0.43	−11.39	−15.94	0.20
Cobb	7.14	19.68	0.20	−12.82	−14.77	0.57
Coweta	0.93	11.93	1.65	−1.27	−14.08	0.85
DeKalb	3.26	16.90	0.98	−5.23	−16.37	0.46
Douglas	2.51	9.99	0.54	−1.41	−12.23	0.60
Fayette	3.39	17.59	0.43	−11.09	−11.69	1.37
Forsyth	3.06	11.40	2.80	−7.14	−9.89	−0.23
Fulton	4.10	13.29	0.56	−9.01	−9.49	0.55
Gwinett	8.30	19.29	0.57	−9.25	−19.39	0.48
Henry	3.66	13.91	2.23	−10.14	−10.49	0.83
Paulding	0.93	5.88	2.47	3.68	−13.29	0.34
Rockdale	2.95	17.87	0.64	−13.67	−8.71	0.91

Land Surface Characterization

The drastic land-use and land-cover change in Atlanta over the past 30 years has resulted in the depletion of the vegetative cover and its replacement by such urban features as residential and commercial buildings, shopping malls, highways, and parking lots. The albedo, temperature, and moisture availability characteristics of the land cover have also been altered. These changes in surface characteristics tended to enhance the contrast in temperatures between the city and its surrounding countryside, a phenomenon known as urban heat island. Urban heat islands can be based on temperature differences that occur in the sub-surface, surface, and air, which are interrelated, although the processes involved in their formation are different (Oke, 1995). Surface heat islands are often greatest by day while those in the air are largest at night. Two types of urban heat islands are normally studied: (1) urban canopy layer (UCL) and (2) urban boundary layer (UBL). The UCL is located beneath the roof and is produced by micro-scale processes operating in the streets ("canyons") between the buildings. The surface temperatures are best used to define it. The UBL is above the roofline, and is a local to meso-scale phenomenon influenced by the general nature of the urban surface. This is best measured using air temperatures between a rural and an urban station.

Surface Temperature Mapping

Landsat TM's band 6 is a thermal-infrared (TIR) band (10.40 to 12.50 μm) that has been commonly used for surface temperature mapping (Nichol, 1994). The surface temperatures extracted are more suitable for the detection of urban heat island at the urban canopy level (UCL). However, Nichol (1996) has found that surface temperatures extracted from Landsat TM TIR data for Singapore closely correspond to ambient air temperatures. More recently, Kawashima *et al.* (2000) have discovered that surface temperatures extracted from Landsat TM data alone explained 80 percent of the observed variation in air temperature during winter nights in Kanto Plain and its surrounding mountainous area, Japan. The relationship seemed to be related to the mean lapse rate of the atmospheric boundary layer. Air temperature was more sensitive to vegetation density

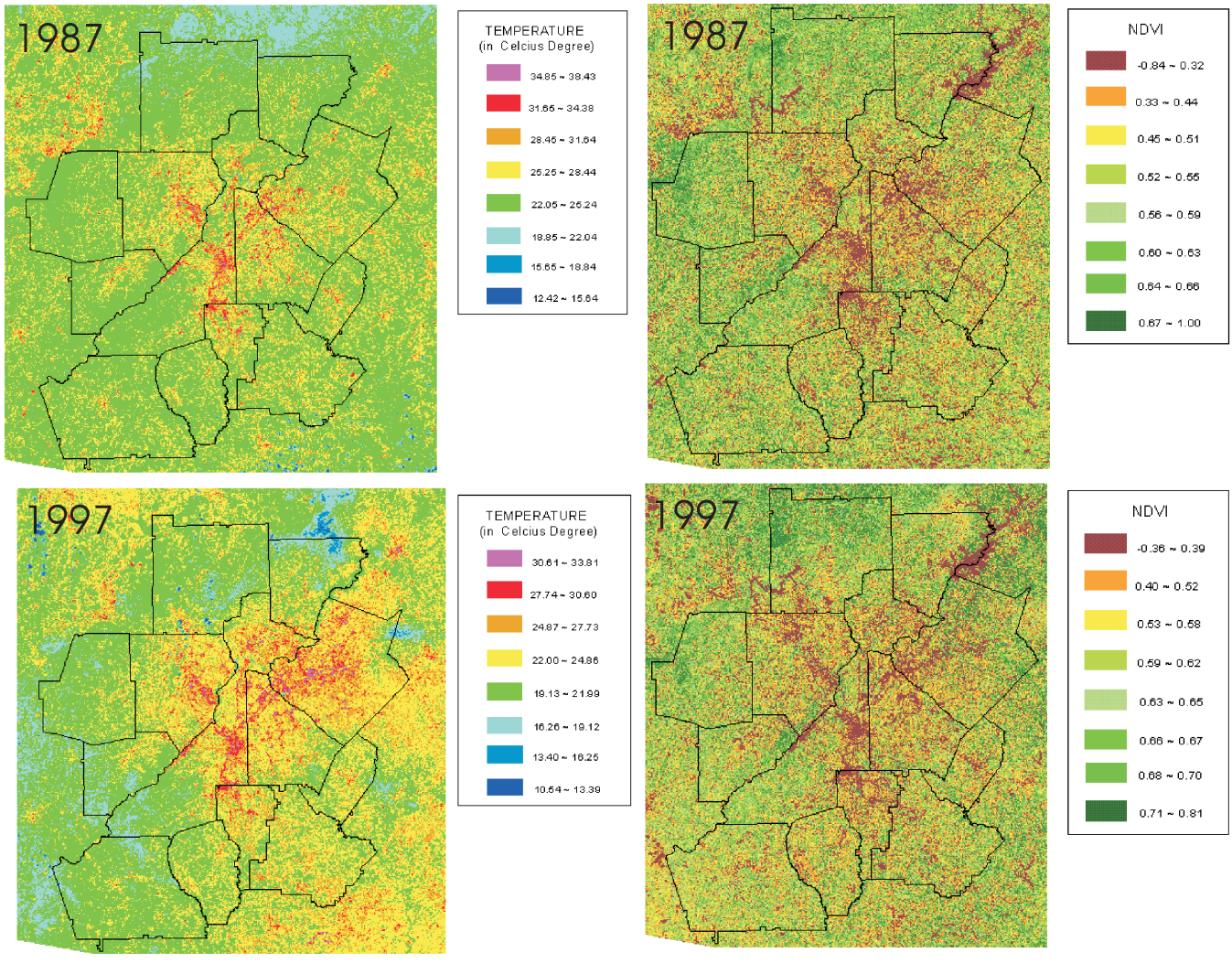

Plate 2. Surface temperature and NDVI maps of Atlanta as extracted from Landsat Thematic Mapper data for 1987 and 1997.

when the mean lapse rate of the atmospheric layer was smaller. It is important to note that surface temperatures reveal not only the boundary conditions of the atmosphere but also the environmental conditions necessary for human beings.

The extraction of surface temperatures from band 6 of Landsat TM data involves first the conversion of the digital number (DN) of the thermal infrared image into apparent temperatures by using a quadratic regression model from Malaret *et al.* (1985) for Landsat 5 TM band 6 data as follows (Nichol, 1994):

$$T(K) = 209.831 + 0.834DN - 0.00133DN^2 \quad (1)$$

where DN is the digital number in 8-bit encoding (0 to 255) and $T(K)$ is absolute temperature in Kelvin. However, the resultant temperatures are blackbody or apparent surface temperatures only and need to be corrected for emissivities of land-cover types.

Using the land-use/land-cover maps obtained from the Landsat TM for 1987 and 1997/1998 (Plate 1) and knowledge of typical emissivities of various common materials for the 8-14 μm range as given by Avery and Berlin (1992), Lillesand and Kiefer (2000), Colwell (1983), and Campbell (2002) (Table 4), an apparent map of emissivities of the different land-use/land-cover classes was produced. This map was then ratioed with the apparent surface temperature map with the following emissivity correction equation to produce the final surface temperature map (Artis and Carnahan 1982):

$$Ts = \frac{T}{1 + \left(\frac{\lambda T}{a}\right) * \ln e} \quad (2)$$

where Ts is the surface temperature in Kelvin (K), T is the blackbody temperatures in Kelvin (K), λ is the wavelength of

TABLE 4. EMISSIVITIES FOR LAND USE AND LAND COVER TYPES USED IN ATLANTA SURFACE TEMPERATURE MAPPING FROM LANDSAT TM THERMAL-INFRARED IMAGE IN THE 8- TO 14-μM RANGE

Land-Use Class	Emissivity
(1) High-Density Urban	0.94
(2) Low-Density Residential	0.95
(3) Cultivated/Exposed Land	0.92
(4) Cropland and Grassland	0.97
(5) Golf Courses and Parks	0.97
(6) Evergreen Forest	0.97
(7) Mixed Forest	0.96
(8) Deciduous Forest	0.95
(9) Water	0.99

emitted radiance in meters, $a = hc/K(1.438*10^{-2}$ mK) where h = Planck's constant ($6.26*10^{-34}$ J · sec), K is the Stefan Bolzmann constant ($1.38*10^{-23}$ J/K), c is the velocity of light ($2.998*10^{8}$ m/sec), and e is emissivity. As a matter of fact, after incorporating the emissivities of the land cover, the difference between *Ts* and *T* was very small. For example, for a blackbody temperature (*T*) of 298 K (25°C) with λ of 11.45 μm, the emissivity-corrected surface temperature (*Ts*) is increased to 298.00569 K (25.00569°C) for $e = 0.90$, and to 298.00165 K (25.00165°C) for $e = 0.97$. Therefore, the blackbody temperatures are just adequate for use in surface temperature mapping from thermal infrared images, thus saving an extra computation step. Two emissivity-corrected surface temperature maps were produced, one for each year, using eight classes divided by the equal interval method (Plate 2). The surface temperatures were higher for the 29 June 1987 scene than for the 10 July 1997 scene with mean temperatures of 24.44°C and 21.79°C, respectively.

From the 1987 surface temperature map, it can be seen that the high temperature areas tended to focus in the inner urban area, spreading out along the highways coinciding with the high-density urban use. Lower temperatures occurred in the "periurban" fringe of the city. The 1997 map shows the amalgamation of some of these high temperature centers forming a larger one. While lower temperatures still occurred in the peripheral counties in the west, high surface temperatures emerged in the northeast and southeast peripheral counties. The county of Gwinnett showed high surface temperatures, which contrasted greatly with those observed in 1987.

The surface temperatures for 1987 and 1997 have also been extracted by counties (Table 5). Both the mean and median values are shown. The mean value in a county tends to be influenced by extreme values. On the other hand, the median value is more stable, and gives extra insight by indicating that 50 percent of the surface temperatures within the county were above or below the median. It is interesting to note that the "hottest" county in 1987 was DeKalb (near the center of the city) (with a mean temperature of 26.23°C and a median temperature of 25.70°C) and the "coolest" county in 1987 was Cherokee at the northern edge (with a mean temperature of 23.46°C and a median temperature of 23.07°C). By 1997, the "hottest" county became Gwinnett (with a mean temperature of 27.23°C and a median temperature of 27.07°C), and the "coolest" county was Cowetta at the southwestern corner (with a mean temperature of 22.67°C and a median temperature of 22.16°C). But in terms of median temperature, the "coolest" county was Paulding (21.93°C), another county at the western border of the Atlanta Metropolitan Area. It is noteworthy that the mean and median temperatures of the "hottest" county were higher in 1997 than in 1987. Similarly, the coolest temperature of the county in 1997 was lower than that in 1987. All these suggest greater contrast in surface temperature in recent years as a result of land-use/land-cover change, and the urban canopy layer (UCL) urban heat island effect.

TABLE 5. SURFACE TEMPERATURES (MEANS AND MEDIANS) OF 1987 AND 1997 BY COUNTIES

No	County	1987 Mean °C	1997 Mean °C	1987 Median °C	1997 Median °C
1	Cherokee	23.46	23.13	23.07	22.84
2	Forsyth	23.85	23.42	23.53	23.19
3	Fulton	25.37	25.43	24.33	24.9
4	Gwinnett	25.43	27.23	24.79	27.07
5	Cobb	25.86	26.06	25.24	25.81
6	Paulding	24.09	22.66	23.87	21.93
7	DeKalb	26.23	26.46	25.7	26.27
8	Douglas	24.39	22.82	23.99	22.16
9	Rockdale	25.00	24.74	24.33	24.44
10	Henry	24.83	25.07	24.33	24.56
11	Clayton	26.01	26.16	25.59	25.81
12	Fayette	24.42	24.01	24.33	23.76
13	Coweta	24.43	22.67	24.33	22.16

The surface temperature maps also revealed the impact of topography on temperatures, most notably the Appalachian Mountain foothill areas to Atlanta's north and east, as well as the Chattahoochee River valley running northwest-southeast along the eastern edge of Atlanta.

Normalized Difference Vegetation Indices (NDVI)

The Normalized Difference Vegetation Index (NDVI) measures the greenness of the environment and the amount of vegetation or the biomass. A higher NDVI indicates a higher degree of greenness and healthy vegetation (Curran, 1980). NDVI can be computed from Landsat MSS and TM data (Jensen, 1996, pp. 179–187). Before NDVI can be computed, the following formula has to be used to convert all digital numbers into radiance values:

$$Radiance = (DN/D_{\max})\,(L_{\max} - L_{\min}) + L_{\max} \quad (3)$$

where L represents radiance (in milliwatts per square centimeter per steradian per micrometer, or symbolically, mW cm^{-2} sr^{-1} mm^{-1}). The subscripts min and max indicate the threshold and saturation values, respectively. *DN* is the digital number of a pixel for a particular band, and $D_{\max}$ is the maximum digital number for a given sensor. $L_{\max}$ and $L_{\min}$ values are published for each band of a given sensor. For Landsat TM, $D_{\max}$ is 255, but for Landsat MSS, it is 127. $L_{\max}$ and $L_{\min}$ for Landsat TM and MSS are available from Markham and Barker (1986).

NDVI from Landsat MSS is computed from the following formula:

$$\text{NDVI} = (\text{MSS5} - \text{MSS7})/(\text{MSS5} + \text{MSS7}) \quad (4)$$

where MSS5 and MSS7 are the red (0.6- to 0.7-μm) and near-infrared (0.8- to 1.1-μm) bands of the Landsat MSS data, respectively.

The NDVI from Landsat TM is computed from the following formula:

$$\text{NDVI} = (\text{TM4} - \text{TM3})/(\text{TM4} + \text{TM3}) \quad (5)$$

where TM3 is band 3, the red band (0.63 to 0.69 μm), and TM4 is band 4, the near-infrared band (0.76 to 0.90 μm), of Landsat TM data.

NDVI values are subject to errors, such as changes in sun angles and sensor viewing angles. Cloud shadows are another problem. Radiometric normalization of image data needs to be carried out before NDVI values are computed.

NDVI values were computed for 1973, 1979, 1983, and 1992 using Landsat MSS data by applying Equation 3, while those for 1987 and 1997 were computed using Landsat TM data by applying Equation 4. The two sets of data may not be totally compatible because of a difference in spatial resolution. All these Landsat data have already been radiometrically normalized as explained under land-use/land-cover mapping.

There is a clear correlation of the NDVI with the month of the year (Table 6). The months of April and May showed lower NDVI values than those for the months of June and July. Higher NDVI values indicate a greater degree of greenness and vegetation amount. It is more useful to compare changes in the NDVI values for 1987 and 1997 because they were calculated from Landsat TM data with a much higher spatial resolution than Landsat MSS data and were acquired at about the same season (29 June 1987 and 29 July 1997, respectively). It is clear that

TABLE 6. SOME STATISTICAL MEASURES FOR THE SIX NDVI MAPS

Landsat Scene Date	min	max	mean	median	mode	Std Dev
13 Apr 1973#	−0.76	1	−0.084	−0.08	−0.07	0.05
11 Jun 1979#	−0.96	0.86	0.44	0.49	0.49	0.19
09 May 1983#	−0.85	0.81	0.28	0.32	0.39	0.19
29 Jun 1987*	−0.88	0.99	0.25	0.30	0.43	0.20
23 Apr 1992#	−0.92	0.77	0.22	0.25	0.31	0.17
29 Jul 1997*	−1.00	0.84	0.32	0.38	0.47	0.20

#calculated using Equation 3 from Landsat MSS data.
*calculated using Equation 4 from Landsat TM data.

the mean, median, and mode of the 1997 NDVI values were higher than those for 1987.

Because the NDVI values are affected by seasons, it is necessary to scale the data to make them comparable. A scaled NDVI value was calculated using the following formula suggested by Gillies *et al.* (1997):

$$NDVI^* = (NDVI - NDVI_{min})/(NDVI_{max} - NDVI_{min}) \quad (6)$$

where NDVI* is the scaled NDVI value, NDVI is the raw NDVI value, $NDVI_{min}$ is the minimum NDVI value, and $NDVI_{max}$ is the maximum NDVI value. The mean scaled NDVI values were calculated and extracted for each county in the Atlanta Metropolitan Area as shown in Table 7. The scaled NDVI values clearly showed particularly low values for 13 April 1973 because of the much colder weather prevailing at that time. On the other hand, the mean scaled NDVI values for the 13 counties in 1979 (11 June 1979) were the highest of all six years. Overall, the variations in NDVI among these 13 counties were small. However, counties in the inner city areas, such as Clayton, Fulton, and DeKalb, exhibited lower NDVI values than did the more peripheral counties such as Paulding, Cherokee, and Coweta. The implication is clearly that the predominantly residential peripheral counties are greener than the commercial inner city counties.

TABLE 7. MEAN SCALED NDVI VALUES BY COUNTIES, 1973–1997

County	1973	1979	1983	1987	1992	1997
Cherokee	0.39	0.80	0.70	0.59	0.70	0.67
Clayton	0.38	0.72	0.64	0.53	0.62	0.62
Cobb	0.38	0.74	0.66	0.55	0.65	0.64
Coweta	0.38	0.78	0.70	0.59	0.67	0.67
DeKalb	0.38	0.73	0.65	0.53	0.64	0.63
Douglas	0.39	0.78	0.69	0.58	0.67	0.67
Fayette	0.38	0.76	0.70	0.57	0.67	0.66
Forsyth	0.38	0.76	0.67	0.55	0.68	0.64
Fulton	0.38	0.75	0.66	0.55	0.66	0.64
Gwinnett	0.39	0.76	0.66	0.55	0.66	0.64
Henry	0.38	0.76	0.69	0.57	0.68	0.66
Paulding	0.39	0.80	0.69	0.60	0.68	0.68
Rockdale	0.39	0.76	0.67	0.57	0.67	0.66

Relationship between NDVI and Surface Temperature Changes

To what extent changes in NDVI are related to surface temperature changes in Atlanta? To answer this question, quantitative mapping of the NDVI and surface temperature change between 1987 and 1997 was performed by using the method of image differencing. The NDVI and surface temperature maps for 1987 were subtracted from the corresponding maps for 1997 (Plate 2). The means and standard deviations were extracted from the two resulting difference maps. By making the following assumption regarding changes, a five-class change map was produced for NDVI and for surface temperature (Table 8):

Class 1: Large decrease (<-2 S.D.)
Class 2: Small decrease (≥ -2 S.D. and <-1 S.D.)
Class 3: No change (≥ -1 S.D. and $\leq +1$ S.D.)
Class 4: Small increase ($>+1$ S.D. and $\leq +2$ S.D.)
Class 5: Large increase ($>+2$ S.D.)

where S.D. is standard deviation. It was found that a large decrease in NDVI during the period 1987 to 1997 was closely related to large increase in surface temperatures. This resulted from the fact that forests were cleared for residential housing tracts. A large percentage of "small increase" in NDVI is related to a small percentage of "small increase" in surface temperatures and *vice versa*. In other words, there is a negative correlative relationship between NDVI values and surface temperatures. This observation is quite well documented in remote sensing literature (e.g., Gallo *et al.*, 1993; Lambin and Ehrlich, 1996).

Atlanta's Urban Heat Island Phenomenon and Health Implications

The surface temperature and NDVI characteristics of Atlanta are the consequences of land-use and land-cover change for the past 30 years. The difference in surface temperatures and NDVI values between the urban and rural areas indicates the difference in surface properties, notably albedo as well as soil thermal and moisture properties, between the two environments that give rise to temperature differences, or urban canopy layer urban heat island phenomenon. It has been shown that there is also a difference in surface temperatures and NDVI values between the inner city counties and peripheral counties. The Atlanta metropolitan area is characterized by a multi-centered development with the emergence of three suburban downtowns along the freeway corridors of I-75, I-85, and I-285, which co-exist with the traditional downtown CBD developed in the 1960s along Peachtree Street with high-rise buildings (Hartshorn and Muller, 1989). As a result, at the microscale, the urban canopy layer urban heat island phenomenon in Atlanta is also multi-centered, with the four downtowns as centers. Research on urban heat island phe-

TABLE 8. NDVI AND SURFACE TEMPERATURE CHANGE (1987–97) COMPARISON

	NDVI Change			Surface Temperature Change		
Change Class	Limits	Area (ha)	%	Limits (°C)	Area (ha)	%
Large decrease	<-0.294	67279.94	2.55	<-4.872	327772.25	12.40
Small decrease	≥ -0.294 to <-0.147	96314.81	3.64	≥ -4.872 to <-2.436	1055944.63	39.96
No change	≥ -0.147 to $\leq +0.147$	1960165.88	74.18	≥ -2.436 to $\leq +2.436$	1198354.69	45.35
Small increase	$>+0.147$ to $\leq +0.294$	389186.81	14.73	$>+2.436$ to $\leq +4.872$	44453.13	1.68
Large increase	$>+0.294$	129524.00	4.90	$>+4.872$	15946.75	0.60
Total		2642471.44	100.00		2642471.44	100.00

nomenon in Atlanta at the mesoscale by Bornstein and Lin (2000) using air temperatures has found daytime and nighttime urban boundary layer urban heat island occurrence. They documented a weak nighttime urban heat island center located slightly northeast of Atlanta on 26 July 1996, a clearly defined nighttime urban heat island centered directly over Atlanta on 30 July 1996, and a strong nighttime urban heat island centered over northeast Atlanta on 03 August 1996. In another research conducted by Dixon (2002), thirty-seven urban heat island initiated precipitation events (i.e., caused by urban-rural temperature difference and related factors) were identified from radar reflectivity data, with weak synoptic flow for the warm season months of May through September for the period from 1996 to 2000. Most of these events occurred during the predawn hours and in the month of July, probably because the urban area was warmer during July than any other months. The positions of these precipitation events were plotted on the land-use and land-cover map for 1997/1998 (Plate 3). It is interesting to note that these events tended to occur near high-density urban areas but outside the I-285 loop, i.e., not in the inner city and the traditional downtown areas. A few events actually occurred around the I-285 loop. A large number occurred in the north in Cherokee county and also northeast in Gwinnett county and the northern part of Fulton County. It is also interesting to note that these precipitation events occurred close to the highways. The research conducted by Bornstein and Lin (2000) indicated that Atlanta's urban boundary layer urban heat island produced a convergence zone that initiated thunderstorms, which were found downwind of the city. Thus, from the location of the precipitation event, one can estimate where the urban heat island is. It was also observed that the Atlanta urban heat island and its urban-induced convergence zone were typical of southern cities in the United States, which was responsible for high ground-level ozone concentrations in the city (McNider *et al.*, 1998). With rapid highway development and the urban sprawl brought about by "periurban" fringe development, it is therefore not surprising that Atlanta has not met the EPA standard of ozone level. A violation occurs when the 8-hour (averaging time) ozone level is greater than or equal to 85 parts per billion (ppb). During the 1996–1998 period, the following counties in Atlanta have recorded ozone levels of greater than 85 ppb: Fulton (113 ppb), Rockdale (107 ppb), De Kalb (102 ppb), Douglas (100 ppb), Gwinnett (95 ppb), and Paulding (94 ppb).

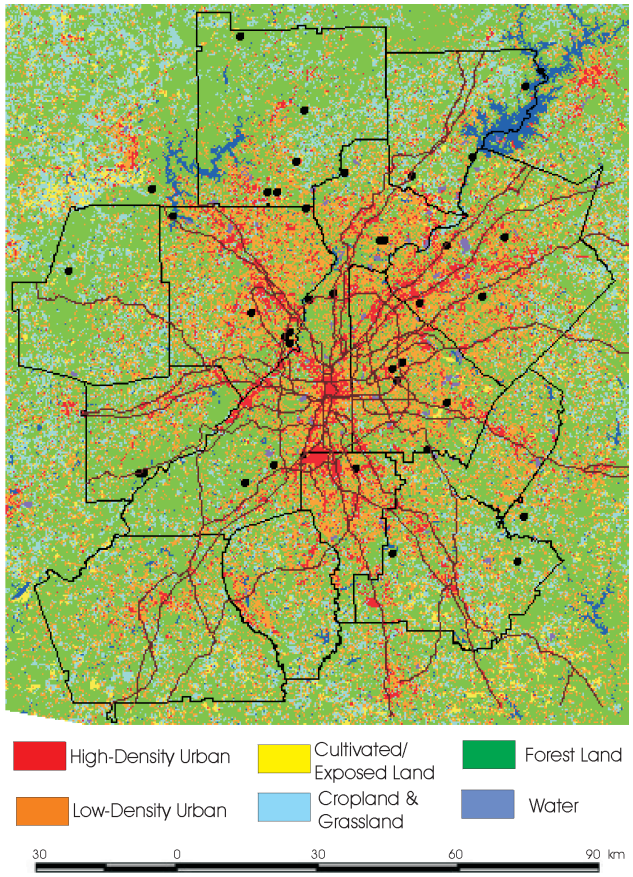

Plate 3. Urban heat island initiated precipitation events in relation to land use and land cover of Atlanta in 1997 (source: Dixon, 2002).

Ground level ozone (O_3), as has been explained earlier (and to be distinguished from stratospheric ozone in the atmosphere, which protects life by blocking harmful ultra-violet radiation from the sun), is created by the reaction between nitrogen oxides (NOx) and volatile organic compounds (VOC) in the presence of sunlight. This makes southern cities worse in the production of ozone, because they are in the Sun Belt and are characterized by higher temperatures, particularly in the summer being stagnant and hot (Chameides and Cowling, 1995). The majority of NO emissions came from transportation sources and fuel combustion. VOC are emitted from a variety sources, including motor vehicles, chemical plants, refineries, factories, consumer and commercial products, and other industrial sources. Ground-level ozone is a significant health hazard. Repeated exposure to ozone pollution may cause permanent damage to the lungs, and can worsen bronchitis, heart disease, emphysema, and asthma (American Lung Association, 2002). It has been reported by the CDC that asthma has increased in importance in the United States during the past 20 years (Mannino *et al.*, 1998). Asthma is a chronic inflammatory disorder of the airways characterized by variable airflow obstruction and airway hyper-responsiveness in which prominent clinical manifestations include wheezing and shortness of breath. Asthma has also been associated with familial infectious, allergenic, socioeconomic, psychosocial, and environmental factors (Weiss *et al.*, 1993; Barbee *et al.*, 1985). It is suspected that ozone pollution is the most important environmental factor that causes asthma, particularly in children (White *et al.*, 1994), as well as being a trigger for hospital emergency room visits (Fauroux *et al.*, 2000). Elderly persons (65 years or older) have also been shown to be at risk through exposure to high ozone and related air pollution levels (MMWR, 1993).

To further investigate the relationship between ground level ozone and its impact on the health of population, annual VOC and NOx emissions of the 13 metropolitan counties of Atlanta for 1996 were mapped, which were then compared with the rates of major cardiovascular diseases and chronic lower respiratory diseases for 1999 (Figure 2). These diseases have been thought to be caused or worsened by ozone pollution. (VOC and NOx data are available from the Environmental Protection Agency (http://www.epa.gov/ttn/naaqs/ozone/areas/sitemap/gacy.htm, last accessed 17 May 2003) while health data are obtained from Georgia Division of Public Health (http://www.ph.dhr.state.ga.us/healthdata/vital.shtml, last accessed 17 May 2003).

The spatial patterns of both the annual VOC and NOx emissions maps exhibited a strong correlation with a Pearson correlation coefficient of 0.98 with $p < 0.0001$. They are identical in that Fulton County had the worst emissions followed by DeKalb, Cobb, and Gwinnett counties in that order. The traditional Atlanta downtown is located in Fulton and DeKalb counties. At least six shopping malls are found in DeKalb

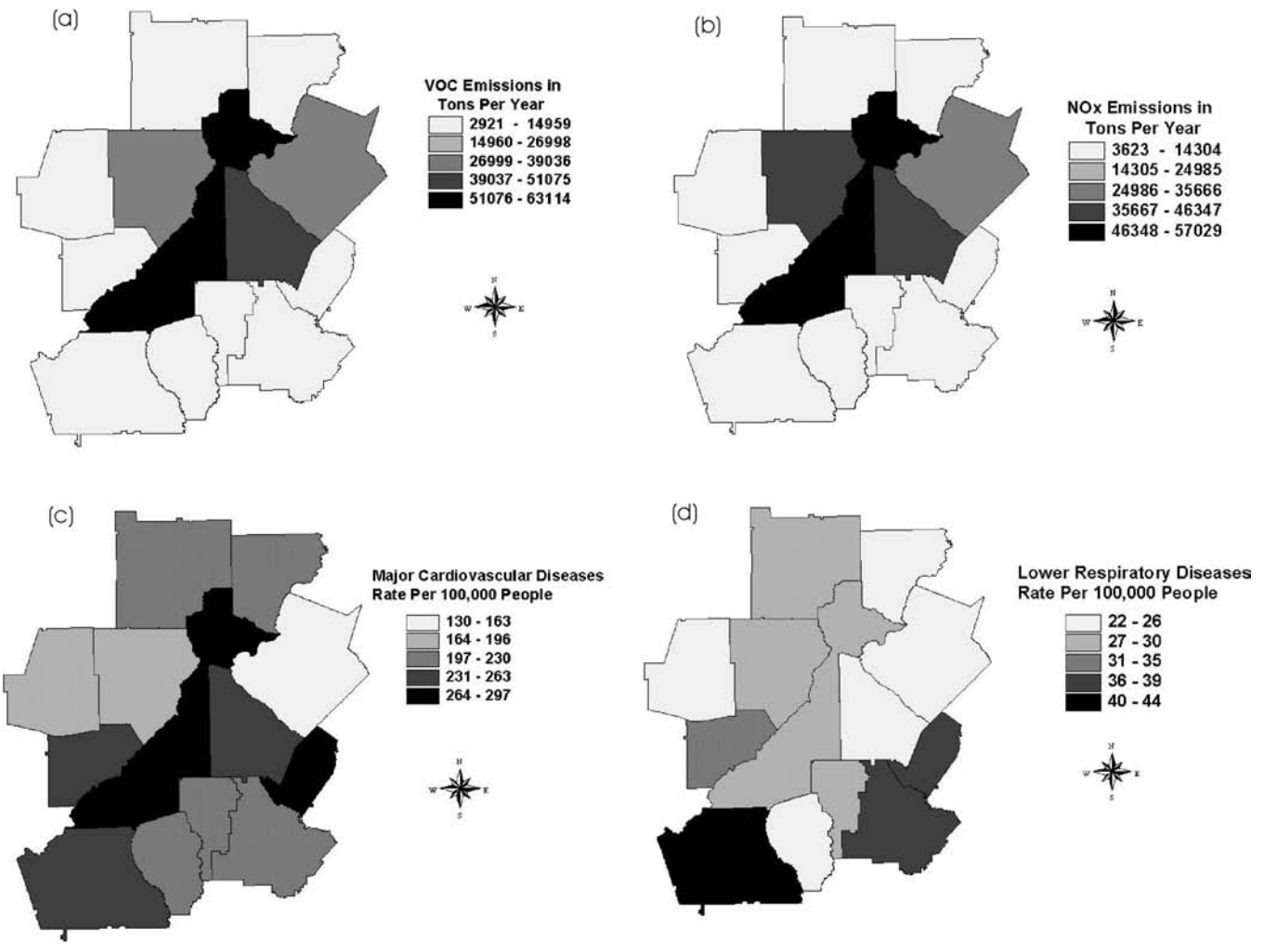

Figure 2. Annual VOC (a) and NOx (b) emissions in relation to major cardiovascular diseases (c) and chronic lower respiratory (d) diseases in Atlanta by counties.

County while Fulton County has five. In Cobb County where Marietta and Smyrna, the two big urban centers, are located, there are two major shopping malls. Gwinnett County is one of the fastest growing counties in the United States, and contains at least one major shopping mall. Interstate highways I-85 and I-285 are found within these counties, and their impacts on the VOC and NOx emissions are great. In the peripheral counties in the north, west, and south, these emissions were much lower. These spatial patterns correlated quite well with that of surface temperatures (Pearson correlation coefficients of 0.66 and 0.64, respectively, with VOC and NOx at $p = 0.01$) and NDVI (Pearson correlation coefficients of -0.60 and -0.56, respectively, with VOC and NOx at $p = 0.03$). In other words, high surface temperatures and low NDVI occurred in Fulton, DeKalb, Cobb, and Gwinnett, while low surface temperatures and high NDVI were found in the peripheral counties (Plate 2, Tables 5 and 7). A canonical correlation was also conducted relating the two biophysical variables (surface temperatures and NDVI) with emissions (VOC and NOx). A first canonical correlation value of 0.67 was obtained, and the canonical redundancy analysis indicated that the proportion of standardized variance explained by the first canonical biophysical variable (i.e., surface temperature) was about 41 percent of the emissions, thus suggesting that biophysical variables would be good predictors of emissions.

The spatial patterns of diseases are less clear-cut in distinguishing between the center and the periphery. Their relation to the two biophysical variables was also investigated using both simple Pearson and canonical correlations. Surface temperatures displayed weak negative correlations with chronic lower respiratory ($r = -0.24$) and cardiovascular diseases ($r = -0.30$), while NDVI showed some correlation with chronic lower respiratory diseases ($r = 0.39$) but no correlation at all with cardiovascular diseases ($r = 0.06$). However, the canonical correlation analysis gave a first canonical correlation value of 0.50, but the canonical redundancy analysis revealed that the first canonical biophysical variable (surface temperature) only explained 8.3 percent of the standardized variance of the disease variables. Therefore, the relationship between these two sets of variables was rather weak.

As for the relationship between the emission and disease spatial patterns, the Pearson correlation showed weak correlation between emissions and chronic lower respiratory diseases only ($r = -0.29$ and $r = -0.19$ for VOC and NOx, respectively). Emissions and cardiovascular diseases were not correlated at all. The canonical correlation analysis gave a first canonical correlation value of 0.76, but the canonical redundancy analysis showed that the first canonical emission variable (VOC) only explained 11.9 percent of the standardized variance of the disease variables. Emissions were not good predictors of

the two types of diseases. Therefore, VOC and NOx seemed to have some weak impact on the health of Atlantans, at least for chronic lower respiratory diseases. These weak relationships may be due to many factors. Apart from air pollution, there are many other causes for cardiovascular and chronic lower respiratory diseases, such as the life style and dietary habits of the population. For example, smoking is an important factor to be considered for all these diseases. Also, the age of the population will have an impact. The chronic lower respiratory diseases will affect mostly the younger and older age groups. Asthma, for example, registered the most substantial increase among children aged 0 to 4 years and persons aged 5 to 14 years based on 1980 through 1994 statistics (Mannino *et al.*, 1998). Another problem may be related to the spatial unit used in the analysis. County may be too coarse as the spatial unit of analysis, and census tract would have been better. Unfortunately, health data are not easily available at fine spatial levels. This type of research in the medical geography field presents a lot of challenges that require our immediate attention. High-resolution satellite remote sensing provides historical and current data on biophysical and land-cover characteristics of the urban environment. It has been confirmed that surface temperature and NDVI are good predictors of VOC and NOx emissions.

Conclusions

For the past 30 years, the Atlanta metropolitan area has undergone dramatic change in land use and land cover that has resulted in loss of forest and cropland, thus drastically altering the land surface characteristics. A time series of Landsat MSS and TM images have been used to map and extract land use and land cover of Atlanta for 1973, 1979, 1983, 1987, 1992, and 1997/1998, using an unsupervised image classification approach supported by reference data acquired from specially flown color-infrared photography and field checks to meet the standard of at least 85 percent in overall, producer's, and user's accuracies. The land-use and land-cover maps revealed a great increase in low-density urban use and high-density urban use at the expense of forest and cropland. The "periurban" fringe counties have received most of the low-density urban use, while high-density urban use tended to develop along the highway corridors of I-85 and I-75 and followed the spread of the population to the urban periphery. To further characterize the land surface that has resulted from these land-use and land-cover changes, Landsat TM thermal band data were used to extract surface temperatures for 1987 and 1997. Normalized difference vegetation indices (NDVI) were also extracted from Landsat MSS and TM images for all the six years under study. Surface temperatures and NDVI exhibited a negative relationship, which suggests that the concrete and asphalt that replaced the forest and cropland increased in areal extent and became hotter while vegetation coverage dwindled and the environment was less green. These modifications of land surface characteristics have promoted the development of urban heat island phenomenon both at the urban canopy and urban boundary layers. A study of urban heat-island-initiated precipitation events in Atlanta during the May to August 1996–2000 period indicated that they tended to occur in high-density urban areas outside the I-285 loop, and most frequently in Cherokee and Gwinnett, with July as the peak month of occurrence. Urban heat island and its urban-induced convergence zone where the precipitation occurs are responsible for high ozone concentration. Ozone pollution causes cardiovascular and chronic lower respiratory diseases. While VOC and NOx emissions, the two ingredients of ground-level ozone, showed distinct differences between the core and the periphery of the city, their effects on cardiovascular and chronic lower respiratory diseases were weak when their spatial patterns of disease incidence rates at the county levels were compared. Other factors, notably demographic, socioeconomic, and life style factors, must have also played an important part in determining causes of these diseases. Future research will need to make use of high quality health statistics or other types of health indicators standardized by age and collected at fine spatial units for such an investigation. On the other hand, canonical correlation analysis has shown that the VOC and NOx emission spatial patterns did show a strong correspondence with the surface temperatures and NDVI spatial patterns derived from satellite images, thus proving that a remote sensing approach for environmental health research is still worthwhile.

Acknowledgments

This research is made possible by research grants #NAS8-97081 and # H-33023D provided by the National Aeronautics and Space Administration (NASA) in connection with Project ATLANTA. Research assistance given by Dr. Xiaojun Yang and Dr. Kai Wang is gratefully acknowledged. The authors wish to thank two anonymous reviewers for comments that helped to improve an earlier draft of the paper.

References

American Lung Association, 2002. *Trends in Air Quality*, Best Practices and Program Services, American Lung Association, http://www.lungusa.org/data/aqp/AQ1.pdf, last accessed 28 May 2003.

Artis, D.A., and W.H. Carnahan, 1982. Survey of emissivity variability in thermography of urban areas, *Remote Sensing of Environment*, 12:313–329.

Avery, T.E., and G.L. Berlin, 1992. *Fundamentals of Remote Sensing and Airphoto Interpretation*, Macmillan, New York, N.Y., 427 p.

Barbee, R.A., R. Dodge, M.L. Lebowitz, and B. Burrows, 1993. The epidemiology of asthma, *Chest*, 87(suppl):21S–25S.

Bornstein, R., and Q. Lin, 2000. Urban heat island and summertime convective thunderstorms in Atlanta: Three case studies, *Atmospheric Environment*, 34:507–516.

Campbell, J.B., 2002. *Introduction to Remote Sensing*, Guilford Press, New York, N.Y., 546 p.

Cardelino, C.A., and W.L. Chameides, 1990. Natural hydrocarbons, urbanization, and urban ozone, *Journal of Geophysical Research*, 95 (D9):13971–13979.

Chameides, W.L., and E.B. Cowling, 1995. *The State of the Southern Oxidant Study (SOS): Policy-Relevant Findings in Ozone Production Research 1988–1994*, College of Forest Resources, North Carolina State University, Raleigh, North Carolina, 136 p.

Changnon, S.A., K.E. Kunkel, and B.C. Reinke, 1996. Impacts and responses to the 1995 heat wave: a call to action, *Bulletin of the American Meteorological Society*, 77(7):1497–1506.

Colwell, R.N. (editor), 1983. *Manual of Remote Sensing, Second Edition*, American Society of Photogrammetry, Falls Church, Virginia, 2440 p.

Curran, P., 1980. Multispectral remote sensing of vegetation amount, *Progress in Physical Geography*, 4:315–341.

Dixon, P.G., 2002. *Climatological Patterns of Atlanta's Urban Heat Island-Initiated Precipitation*, M.S. thesis, Department of Geography, University of Georgia, Athens, Georgia, 168 p.

Fauroux, B., M. Sampil, P. Quénel, and Y. Lemoullec, 2000. Ozone: A trigger for hospital pediatric asthma emergency room visits, *Pediatric Pulmonology*, 30:41–46.

Gallo, K.P., A.L. McNab, T.R. Karl, J.F. Brown, J.J. Hood, and J.D. Tarpley, 1993. The use of a vegetation index for assessment of the urban heat island effect, *International Journal of Remote Sensing*, 14(11): 2223–2230.

Gillies, R.R., T.N. Carlson, J. Cui, W.P. Kustas, and K.S. Humes, 1997. A verification of the 'triangle' method for obtaining surface soil water content and energy fluxes from remote measurements of the Normalized Difference Vegetation Index (NDVI) and surface radiant temperature, *International Journal of Remote Sensing*, 18(15):3145–3166.

Hall, F.G., D.E. Strebel, J.E. Nickeson, and S.J. Goetz, 1991. Radiometric rectification: Toward a common radiometric response among

multidate, multisensor images, *Remote Sensing of Environment*, 35:11–27.

Hartshorn, T.A., and P.O. Muller, 1989. Suburban downtowns and the transformation of metropolitan Atlanta's business landscape, *Urban Geography*, 10:375–395.

Jensen, J.R., 1996. *Introductory Digital Image Processing: A Remote Sensing Perspective*, Prentice-Hall, Upper Saddle River, New Jersey, 316 p.

Kawashima, S., T. Ishida, M. Minomura, and T. Miwa, 2000. Relations between surface temperature and air temperature on a local scale during winter nights, *Journal of Applied Meteorology*, 39:1570–1579.

Kostmayer, P.H., 1989. The American landscape in the 21st century, *Congressional Record*, 135, 18 May, p. 9963.

Lambin, E.F., and D. Ehrlich, 1996. The surface temperature-vegetation index space for land cover and land-cover change analysis, *International Journal of Remote Sensing*, 17:463–487.

Lillesand, T.M., and R.W. Kiefer, 2000. *Remote Sensing and Image Interpretation, Third Edition*, John Wiley and Sons, New York, N.Y., 724 p.

Malaret, E., L.A. Bartolucci, D.F. Lozano, P.E. Anuta, and C.D. Mcgillem, 1985. Landsat-4 and Landsat-5 Thematic Mapper data quality analysis, *Photogrammetric Engineering & Remote Sensing*, 51: 1407–1416.

Mannino, D.M., D.M. Homa, C.A. Pertowski, A. Ashizawa, L.L. Nixon, C.A. Johnson, L.B. Ball, E. Jack, and D.S. Kang, 1998. Surveillance for asthma—United States, 1960–1995. *Morbidity and Mortality Weekly Report*, Centers for Disease Control, 24 April 1998, 47(SS-1): 1–28 (wysigyg://14/http://www.cdc.gov/mmwr/preview/mmwrhtml/00052262.htm, last accessed 17 May 2003).

Markham, B.L., and J.L. Barker, 1986. Landsat MSS and TM post-calibration dynamic ranges, exoatmospheric reflectance, and at-satellite temperatures, *Landsat Technical Notes*, No. 1, pp. 3–8.

McNider, R.W., N.A. Song, S. Mueller, and R. Bornstein, 1998. The role of convergence zones in producing extreme concentration events, 10th Joint AMS/AWMA Conference on the Applications of Air Pollution Meteorology, 11–16 January, Phoenix, Arizona (American Meteorological Society, Boston, Massachusetts), Preprint Volume, Paper 3.4.

MMWR, 1993. Populations at risk from air pollution—United States, 1991, Report on "Health Objectives for the Nation," *Morbidity and Mortality Weekly Report*, 42(16):301–304.

_____, 1995. Heat-related mortality—Chicago, July 1995, *Morbidity and Mortality Weekly Report*, 44(31):577–579.

Nichol, J.E., 1994. A GIS-based approach to microclimate monitoring in Singapore's high-rise housing estates, *Photogrammetric Engineering & Remote Sensing*, 60:1225–1232.

_____, 1996. High-resolution surface temperature pattern related to urban morphology in a tropical city: a satellite-based study, *Journal of Applied Meteorology*, 35:135–146.

Oke, T.R., 1995. The heat island of the urban boundary layer: Characteristics, causes and effects, *Wind Climate in Cities* (J.E. Cermak, A.G. Davenport, E.J. Plate, and D.X. Viegas, editors), Kluwer Academic Publishers, Dordrecht, The Netherlands, pp. 81–107.

Research Atlanta, Inc., 1993. *The Dynamics of Change: An Analysis of Growth In Metropolitan Atlanta Over The Past Two Decades*, Policy Research Center, Georgia State University, Atlanta, Georgia, 82 p.

Sailor, D.J., 1995. Simulated urban climate response to modifications in surface albedo and vegetative cover, *Journal of Applied Meteorology*, 34(7):1694–1704.

Weiss, K.B., P.J. Gergen, and D.K. Wagener, 1993. Breathing better of wheezing worse? The changing epidemiology of asthma morbidity and mortality, *Annual Review of Public Health*, 14:491–513.

White, M.C., R.A. Etzel, W.D. Wilcox, and C. Lloyd, 1994. Exacerbation of childhood asthma and ozone pollution in Atlanta, *Environmental Research*, 65(1):56–68.

Yang, X., and C.P. Lo, 2000. Relative radiometric normalization performance for change detection from multi-date satellite images, *Photogrammetric Engineering & Remote Sensing*, 66(8):967–980.

_____, 2002. Using a time series of satellite imagery to detect land use and land cover changes in the Atlanta, Georgia metropolitan area, *International Journal of Remote Sensing*, 23:1775–1798.